REDUCTION OF $X-Y$ COUPLING EFFECT IN THE SUPER-ALIS COMPACT STORAGE RING

KOJI YAMADA * and TERUO HOSOKAWA

*System Electronics Laboratories, Nippon Telegraph and Telephone
Corporation (NTT), 3-1 Morinosato-wakamiya, Atsugi, 243-01 Japan*

The $x-y$ coupling effect, especially the tilt of the beam profiles, was effectively reduced in the Super-ALIS compact electron storage ring. It is determined that the origin of the coupling is the vertical closed orbit distortion in the sextupole field of the super-conducting bending magnets. The method for coupling reduction is derived from the harmonic analysis of the fundamental-coupling matrix introduced by Peggs. The main feature of this method is the suppression of the most harmful Fourier components of the skew-quadrupole perturbation using just one or two thin skew-quadrupole magnets.

Keywords: Storage ring; Synchrotron; Coupling; Sextupole field; Closed orbit distortion; Betatron tune; Beam profile; Superconducting magnet; Skew-quadrupole magnet

1 INTRODUCTION

In storage rings for synchrotron radiation (SR), the sextupole magnetic field exists as a stray field in the bending magnets (BM) or sextupole magnets for chromaticity correction. It is known that as well as the original sextupole perturbation, beams passing through a vertical off-centered orbit also experience skew-quadrupole perturbation whose strength is $2k_s \Delta y$, where k_s and Δy are the strength of the sextupole field and the vertical distance from the center of the field. The skew-quadrupole perturbation couples the horizontal and vertical motions of the beams and generally tilts the axes of the normal

---

* Corresponding author.

modes to the ordinary horizontal or vertical axes.[1,2] This phenomenon results in the tilting of beam profiles.

Such tilted beam profiles are undesirable for experiments using SR. In X-ray lithography beamlines, the tilting of beam profiles seriously degrades the uniformity of exposure. In beamlines using monochromators, the intensity of the X-rays is decreased because the slit of the monochromator must be narrow to obtain a fine resolution.

This problem is more serious in recently developed compact storage rings[3–5] because most of these compact rings use superconducting bending magnets that generally have a large sextupole field. Moreover, in superconducting compact storage rings, the closed orbit distortion is likely to become enlarged because of the following factors. In superconducting magnets, the median plane of the magnetic field is determined by the shape and position of the coils rather than by the yoke geometry; therefore, the median plane of the field might be displaced from the geometrical median of the magnet that is the reference of the magnet alignment. Additionally, restrictions in the number of steerers and position monitors make corrections of closed orbits difficult in compact rings.

The serious coupling effect was observed also in the Super-ALIS superconducting compact storage ring,[6] and the quality of SR beams was degraded. To eliminate this problem, in this work, we analyze the coupled betatron motions theoretically and derive an effective method for reducing coupling effect that is suitable for compact rings. Then, we confirm the validity of this method in Super-ALIS.

2   THEORETICAL APPROACH

From harmonic analysis of the fundamental coupling matrix H introduced by Peggs,[1] we obtain a method for coupling reduction. For the analysis, we use the coordinate system $X = (x, x', y, y')$ obtained by transforming the physical coordinate system $Y = (x, x', y, y')$ through Courant–Snyder transformation.[7] For simplicity, the phase parameters are assumed to be $\phi_x = \phi_y = \phi$ although ϕ_x and ϕ_y are slightly different in the X system. This assumption is reasonable because the higher harmonic components excited by the small difference between ϕ_x and ϕ_y are not significant in the harmonic analysis to be discussed in this work.

Transforming the sum form of the H matrix given by Peggs into an integral of ϕ, the matrix at the arbitrary phase position ϕ_P can be rewritten as

$$
\begin{aligned}
H(\phi_P) \sim & \frac{C}{2\pi} \int_0^{2\pi} g(\phi - \phi_P) \\
& \times \Bigg\{ R(2\pi Q_x)R(-(\phi - \phi_P)Q_x)\begin{pmatrix} 0 & 0 \\ 1 & 0 \end{pmatrix} R((\phi - \phi_P)Q_y) \\
& - R(-(\phi - \phi_P)Q_x)\begin{pmatrix} 0 & 0 \\ 1 & 0 \end{pmatrix} R((\phi - \phi_P)Q_y)R^{-1}(2\pi Q_y) \Bigg\} \, d\phi,
\end{aligned}
$$

$$(1)$$

where $R(\theta)$ is the 2×2 rotation matrix and Q_x, Q_y are the betatron tunes in the x and y motions, respectively. C is the circumference of the ring. $g(\phi)$ is the azimuthal distribution of the normalized skew-quadrupole perturbation and is expressed by

$$
g(\phi) = \sqrt{\beta_x(\phi)\beta_y(\phi)} \frac{(\partial B_x(\phi)/\partial x)}{(B\rho)}, \tag{2}
$$

where $\partial B_x/\partial x$ is the gradient of the skew-quadrupole component and $(B\rho)$ is the momentum of electrons measured in the unit of the elemental charge "e". Here, $g(\phi)$ has a period of 2π; therefore, it can be expanded into a Fourier series:

$$
g(\phi) = \sum_{k=-\infty}^{+\infty} g_k e^{ik\phi}, \tag{3}
$$

where k is the wave number and g_k is the kth Fourier component. Using the following relation of the Fourier expansion

$$
g(\phi - \phi_P) = \sum_{k=-\infty}^{+\infty} g_k e^{-ik\phi_P} e^{ik\phi}, \tag{4}
$$

we can obtain the following equation for $H(\phi_P)$:

$$
H(\phi_P) \sim \sum_{k=-\infty}^{+\infty} \frac{Cg_k e^{-ik\phi_P}}{2\pi} \int_0^{2\pi} e^{ik\phi}\{\ldots\} \, d\phi. \tag{5}
$$

In this equation $\{\dots\}$ represents the same bracketed term as that used in Eq. (1). The integral operation in this equation is similar to that used in obtaining the kth Fourier component of the terms inside the bracket. Therefore, $H(\phi_P)$ is a zero matrix unless the skew-quadrupole perturbation has the same Fourier components as the bracket term.

We can easily calculate the terms inside the bracket and obtain the simple result that the terms only have the wave numbers of $\pm(Q_x - Q_y)$ and $\pm(Q_x + Q_y)$. We show here only $(1, 1)$ element of this matrix as

$$
\begin{aligned}
\{\dots\}_{11} = [&\sin\{+(Q_x - Q_y)\phi + (Q_x - Q_y)\phi_P + 2\pi Q_y\} \\
+ &\sin\{-(Q_x - Q_y)\phi - (Q_x - Q_y)\phi_P + 2\pi Q_x\} \\
+ &\sin\{+(Q_x + Q_y)\phi + (Q_x + Q_y)\phi_P - 2\pi Q_y\} \\
+ &\sin\{-(Q_x + Q_y)\phi - (Q_x + Q_y)\phi_P + 2\pi Q_x\}]/2. \quad (6)
\end{aligned}
$$

Consequently, $H(\phi_P)$ can become a non-zero matrix only when the following conditions are fulfilled:

$$
k \sim \pm(Q_x - Q_y) \quad \text{or} \quad k \sim \pm(Q_x + Q_y). \quad (7)
$$

In many SR rings, the first of those conditions is more significant than the latter because the rings are often operated near the difference resonances which are represented by expressions similar to this condition. The difference resonance results only in the beats between the x and y motions and does not cause a loss of beam; therefore, we often use it to increase the coupling constant for the long beam lifetime. The sum resonance, however, must be avoided because it results in an infinite emittance growth and leads to a loss of beam.[8]

Thus, we have reached an important result: the coupling effect appears only when the wave number of the azimuthal distribution of the skew-quadrupole perturbation is close to the difference of the horizontal and vertical tunes. The result is similar to the one derived by Bruck.[9]

This result gives an effective method for coupling reduction. The coupling effects can be greatly reduced by suppressing only Fourier components $g_{\pm k_d}$ where k_d is a natural number close to the absolute value of the tune difference. Other components do not have to be

considered. The method can ideally be achieved by adding thin (or δ-like) skew-quadrupole lenses. Generally, this method requires only two skew-quadrupole lenses because the Fourier components to be suppressed are those with wave numbers $+k_d$ and $-k_d$.

We should note that the number of additional lenses can be reduced to just one. The Fourier series on $g(\phi)$ can also be defined as

$$g(\phi) = f_0 + \sum_{k=1}^{+\infty} f_k \cos(k(\phi - \Delta\phi_k)), \qquad (8)$$

where $f_0 = g_0$, $f_k = 2\sqrt{g_k g_{-k}} = 2|g_k|$ and $\Delta\phi_k$ is the initial phase. This equation means that the simultaneous control of the $+k_d$ and $-k_d$ components of $g(\phi)$ can be equivalent to controlling the amplitude f_{k_d} and the phase ϕ_{k_d} in Eq. (8). The control of the phase can be interpreted as selecting the position of the skew-quadrupole lens along the orbit; therefore, even one skew-quadrupole lens can suppress the $+k_d$ and $-k_d$ components simultaneously if we can select a suitable position for the lens. The position and the strength of the lens can be determined by the following method. Using Poisson's sum rule, the periodic δ function with the period of 2π and the strength k_{lens} can be expanded into the following Fourier series:

$$k_{lens} \sum_{n=-\infty}^{\infty} \delta(\phi - \phi_{lens} - 2n\pi) = k_{lens}\left\{ \frac{1}{2\pi} + \frac{1}{\pi}\sum_{k=1}^{\infty}\cos(k(\phi - \phi_{lens})) \right\}, \quad (9)$$

where ϕ_{lens} is the phase corresponding to the position of the lens. The coupling is reduced when the k_d component of this δ-like lens suppresses the k_d component originating from the undesirable skew-quadrupole perturbation:

$$f_{k_d}\cos(k_d(\phi - \Delta\phi_{k_d})) + \frac{k_{lens}}{\pi}\cos(k_d(\phi - \phi_{lens})) = 0. \qquad (10)$$

One of the solutions of this equation is

$$k_{lens} = -\pi f_{k_d} \quad \text{and} \quad \phi_{lens} = \Delta\phi_{k_d}. \qquad (11)$$

The solution means that a lens with strength $-\pi f_{k_d}$ is located at a position where the perturbation of the k_d component originating

from the undesirable skew-quadrupole force is maximum. It can also be a solution that a πf_{k_d} strength lens is located at a position where the undesirable skew-quadrupole force is minimum.

To sum up, one advantage of this method is that only one or two skew-quadrupole lenses are needed for coupling reduction. Another significant advantage is that the coupling reduction is effective all over the orbit. This characteristic is easily proven by g_k in Eq. (5) being independent of ϕ_P. These advantages are very important, particularly in compact rings that have little space for additional instruments.

3 COUPLING BEHAVIOR IN SUPER-ALIS

3.1 Super-ALIS and the Source of the Coupling

Super-ALIS is a superconducting electron storage ring for SR.[3] The schematic of this machine is shown in Figure 1 and the betatron functions are shown in Figure 2. The machine parameters are shown in Table I. This machine has two superconducting 180-degree bending magnets, BM1 and BM2. The magnets have a maximum magnetic field of 3.0 T. The uniformity of the field is not much better than that of normal-conducting magnets. Therefore, the BMs in Super-ALIS have correction coils for multipole fields.

The measured magnetic field at the center of BM1 excited to 3.0 T is shown in Figure 3(a). The solid line in this figure is the field without correction coils. Figure 4 shows the sextupole components along the orbit in BM1. The sextupole component $\partial^2 B_y / 2 \partial x^2$ is about $-1.8\,\text{T/m}^2$, except at the edges. At the edges, the field distribution is quite different, as shown in Figure 3(b). The sextupole field without correction coils does not affect the dynamic aperture very much. For the coupling effect, however, tracking simulations show that only a

TABLE I   Super-ALIS machine parameters

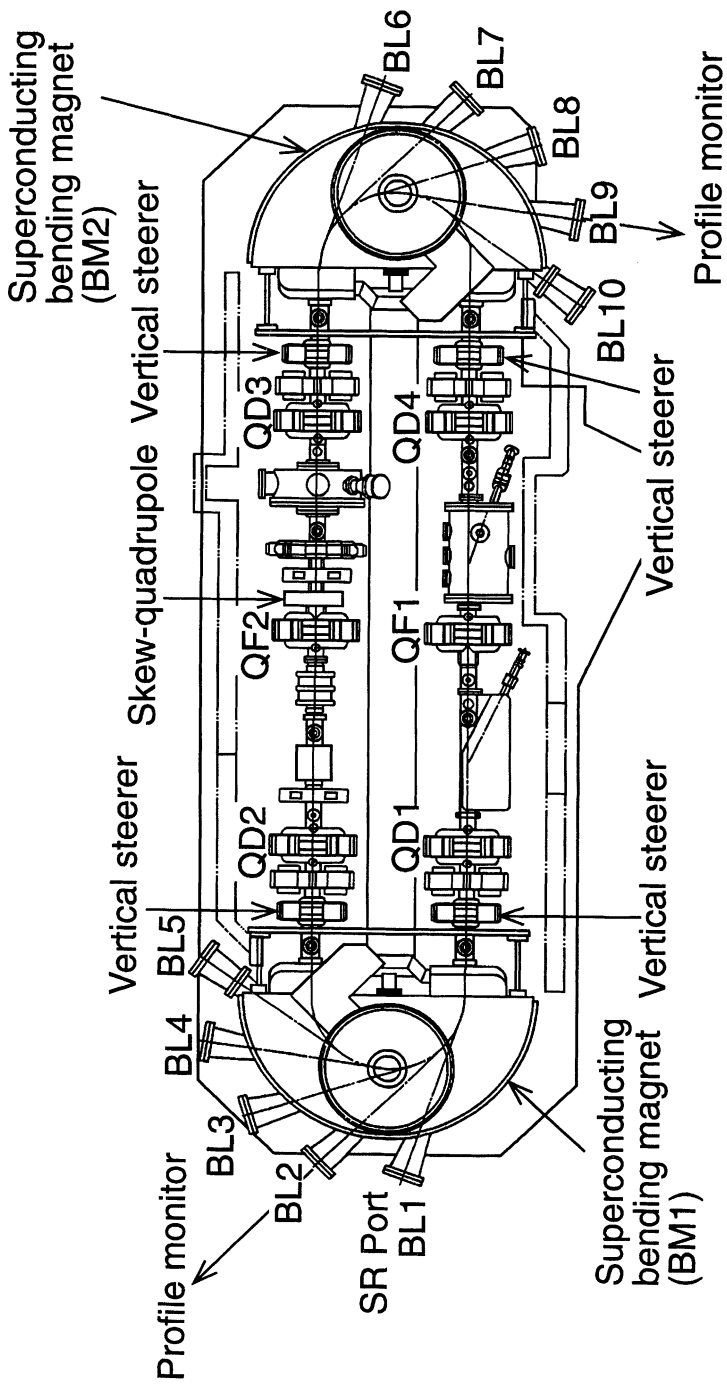|	
Max. energy	600 MeV
Max. bending field	3.0 T
Type of BMs	superconducting (with iron core and yoke)
Betatron tune	$Q_x = 1.585$, $Q_y = 0.583$
Transverse emittance	$9.5 \times 10^{-7}\pi\,\text{m rad}$
Circumference	16.8 m

Superconducting bending magnet (BM2)

Vertical steerer

Skew-quadrupole

Vertical steerer

Profile monitor

BL6
BL7
BL8
BL9
BL10

QD3
QD4

QF2
QF1

QD2
QD1

BL5

Vertical steerer

BL4
BL3
BL2
BL1
SR Port

Profile monitor

Superconducting bending magnet (BM1)

Vertical steerer

FIGURE 1   The superconducting storage ring Super-ALIS.

BM1 QD2 QF2 QD3 BM2 QD4 QF1 QD1 BM1
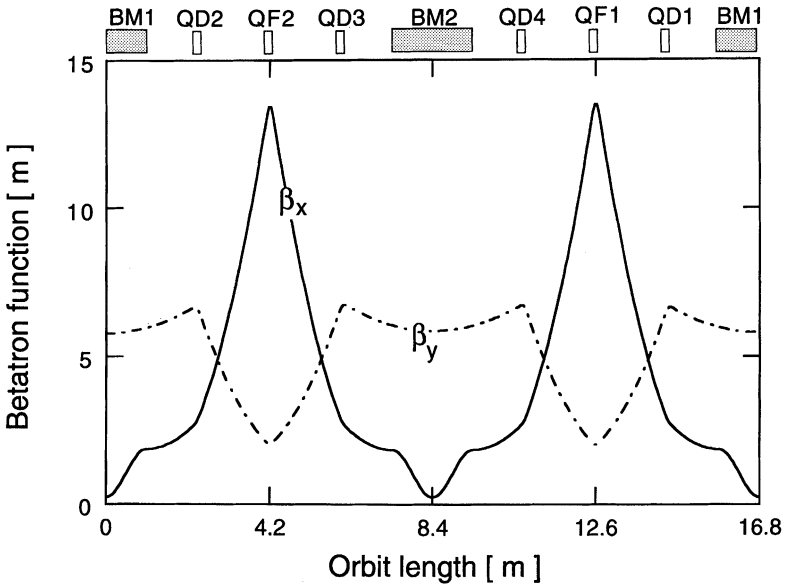
FIGURE 2   Betatron functions of Super-ALIS.

vertical closed orbit distortion of 1 mm in the sextupole field gives serious coupling effects to the 600-MeV beams in Super-ALIS's routine operation.

By using correction coils, the sextupole components can be reduced to about 1/10 (except at the edges) as shown by the dotted lines in Figures 3(a) and 4. At the edges, however, the sextupole components become large even if the correction coils are used, as shown by the dotted line in Figure 3(b).

3.2   Observation of Coupling Effect

3.2.1   *Monitoring System*

At least two monitoring systems are needed to observe the coupling behavior in Super-ALIS, because our goal is to eliminate the tilt of beam profiles in both BMs. One monitoring system is installed in BM1 and the other in BM2. For the monitor in BM2, we employ the BL9 SR port. The SR light extracted from the port is focused on a CCD camera. For the monitor in BM1, we make use of the X-ray
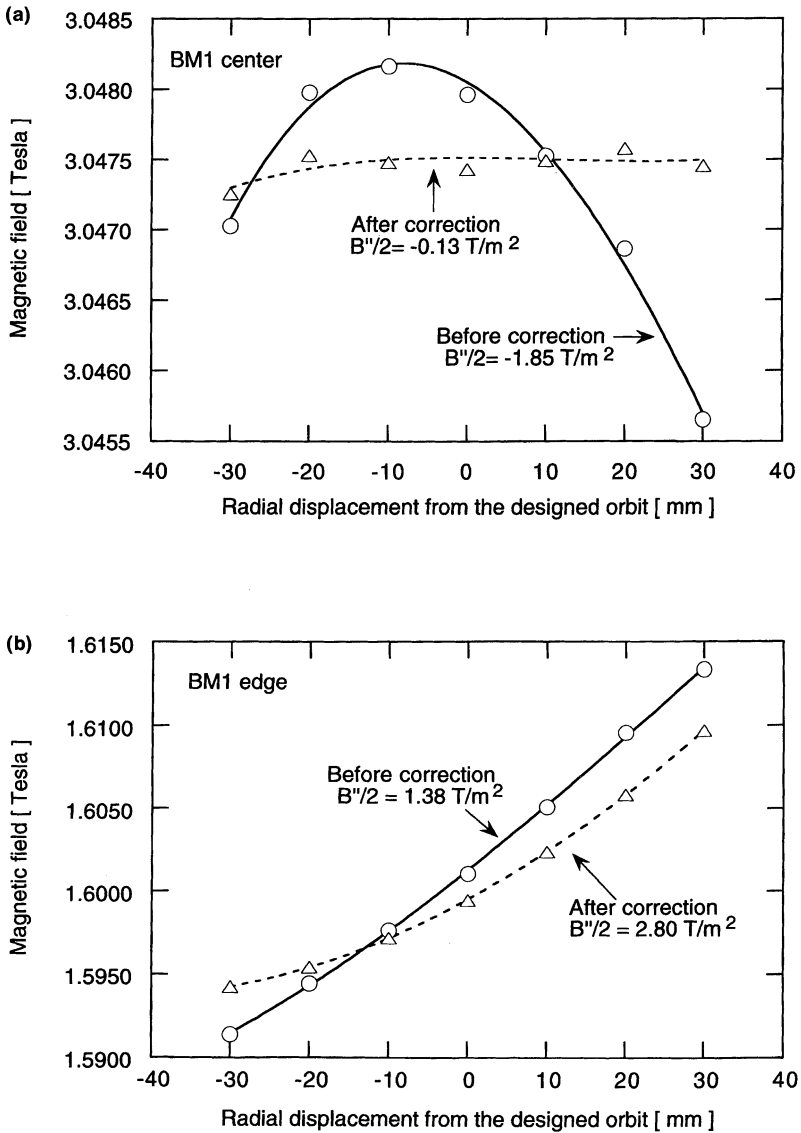
(a)

BM1 center

After correction
B"/2= -0.13 T/m^2

Before correction →
B"/2= -1.85 T/m^2

Magnetic field [Tesla]

Radial displacement from the designed orbit [mm]

(b)

BM1 edge

Before correction
B"/2 = 1.38 T/m^2

After correction
B"/2 = 2.80 T/m^2

Magnetic field [Tesla]

Radial displacement from the designed orbit [mm]

FIGURE 3   Radial distribution of the magnetic field on the median plane of BM1: (a) at the center and (b) at the entrance edge.
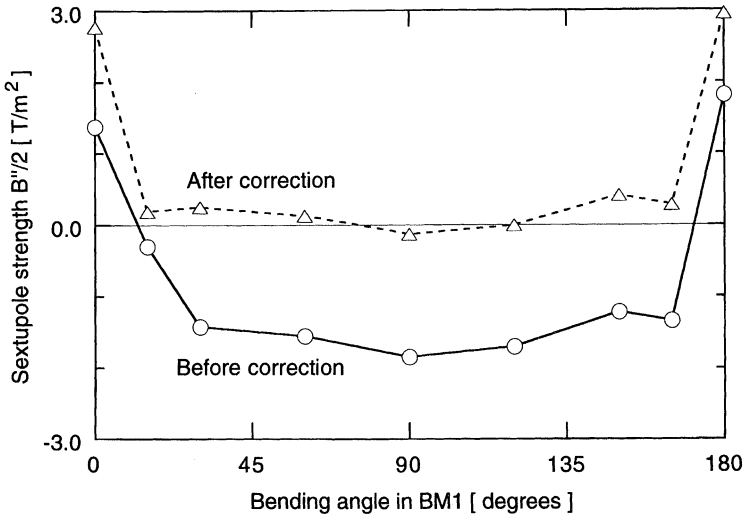
FIGURE 4   Sextupole components of BM1 along the designed central orbit.

lithography beamline[10] installed in the BL2 SR port, as shown
in Figure 5. In this beamline, X-ray beams are collimated by two
toroidal mirrors (M1 and M2) and guided to the exposure plane. To
monitor the beam profile, we use a pinhole screen located upstream
of M1 and adjusted to the axis of the beamline optics. The image of
the beam profile is observed on a luminescent screen located down-
stream of M1. Though M1 is a toroidal mirror, the image on the
luminescent screen shows almost the correct profile because the beam
spot through the pinhole is very small on M1 and is precisely adjusted
to the optical axis.

3.2.2   Reference Orbit

In Super-ALIS, vertical displacements might exist between the median
plane of beam position monitors, which are installed in the vacuum
duct, and the median of the magnetic field of BMs. The displace-
ments originate from two factors. One is that the median plane of the
magnetic field is determined by the shape and position of the coils
rather than by the yoke geometry of BMs. The other is that the heavy
BMs (25 tons each) sink unevenly over the years while the other
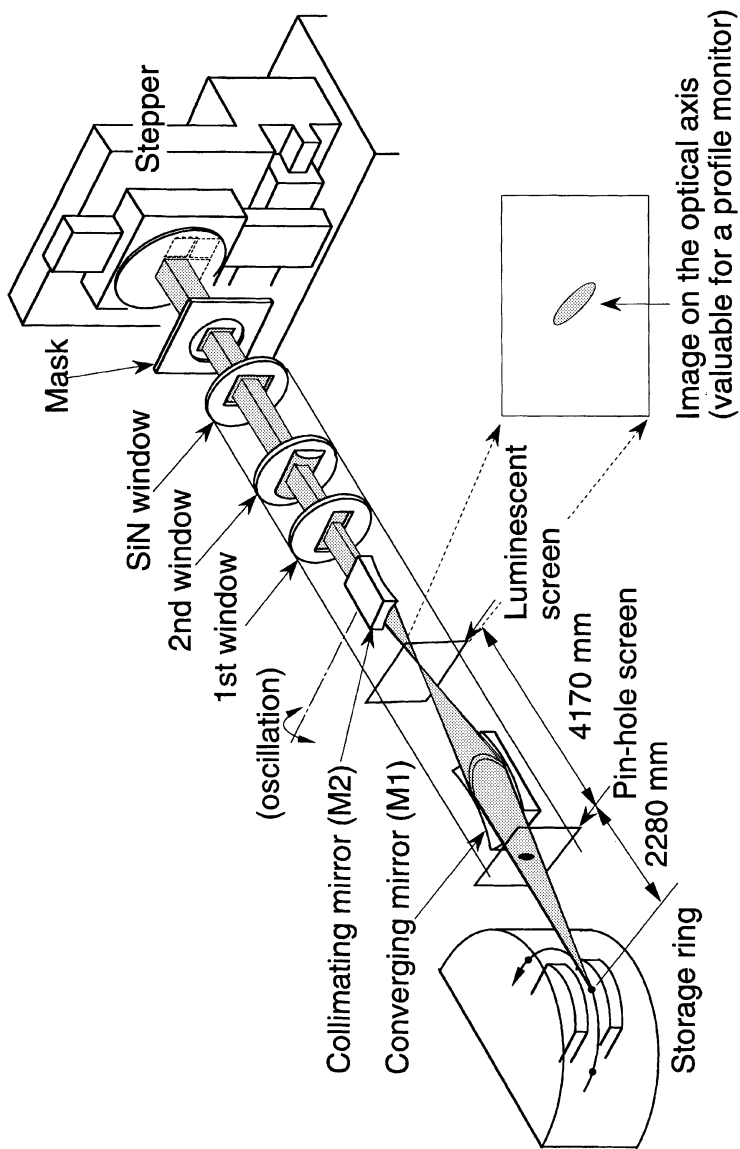components stay at their original levels.

FIGURE 5   Schematic of the lithography beamline as a profile monitor on BL2.

We confirmed the displacements by observing the beam profiles
under the condition where the vertical closed orbit defined as the
reading of the position monitors was adjusted to nearly zero and the
sextupole field in the BMs was not corrected. In an ideal machine,
this condition should give flat beam profiles; however, the experi-
ment resulted in tilted profiles. This means the closed orbit defined as
the reading of position monitors cannot give correct orbit displace-
ments in BMs. Therefore, we cannot estimate correct coupling effects
as 'ong as we use the closed orbit defined by this scheme.

To eliminate this problem, we introduced a reference orbit that
gave no coupling. To determine this orbit, we searched for a vertical
closed orbit giving flat beam profiles by adjusting the vertical steer-
ers, and found the reference orbit shown in Figure 6. Here, we rede-
fine a vertical closed orbit as the orbit displacement from the
reference orbit. All the closed orbits mentioned in the following sec-
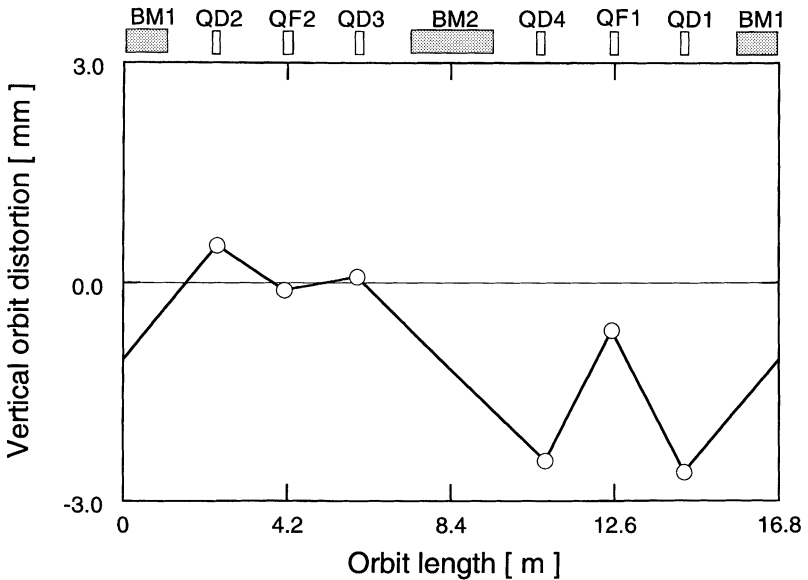tions are defined this way.

FIGURE 6   Reference vertical orbit.

3.2.3 *Estimation of the Coupling Behavior*

Prior to observing the coupling effects, we estimate the coupling effects originating from the vertical closed orbit distortions in the sextupole field of BMs. We assume four types of closed orbits obtained by exciting four vertical steerers. These closed orbits are represented by the letters A through D, as shown in Figure 7.

Figures 8(a)–(d) are the calculated skew-quadrupole perturbations originating from these closed orbit distortions in the sextupole field of BMs without using correction coils. The coupling effect is mainly caused by the $k = 1$ component of the skew-quadrupole perturbation because the wave number is close to the difference of the tunes in Super-ALIS. Therefore, only perturbations of $k = 1$ components are extracted from the original skew-quadrupole perturbations; they are shown in these figures by chained lines.

From these calculated $k = 1$ components, we can predict the coupling behavior. For example, in such a case that the enlargement of the vertical beam size is not observed significantly (or $d_{12} \sim 0$ in Eq. (13)), the tilt angles in the Y system are roughly estimated by the following
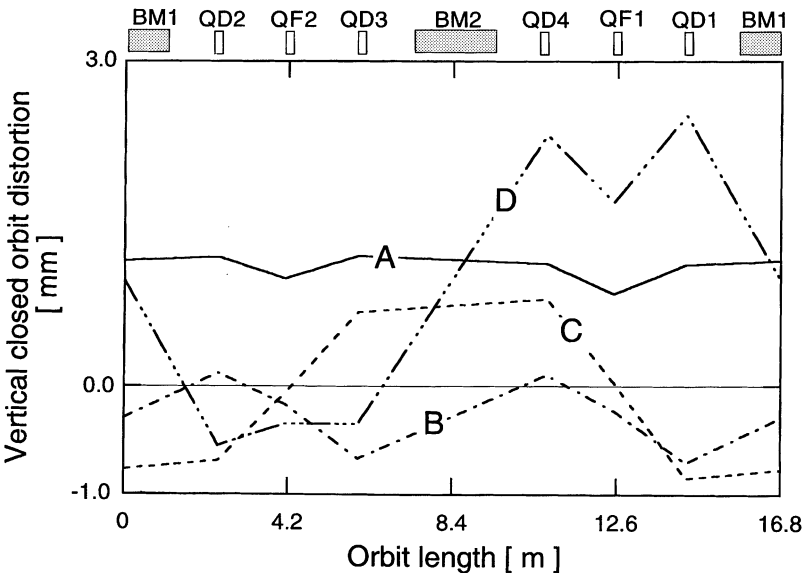

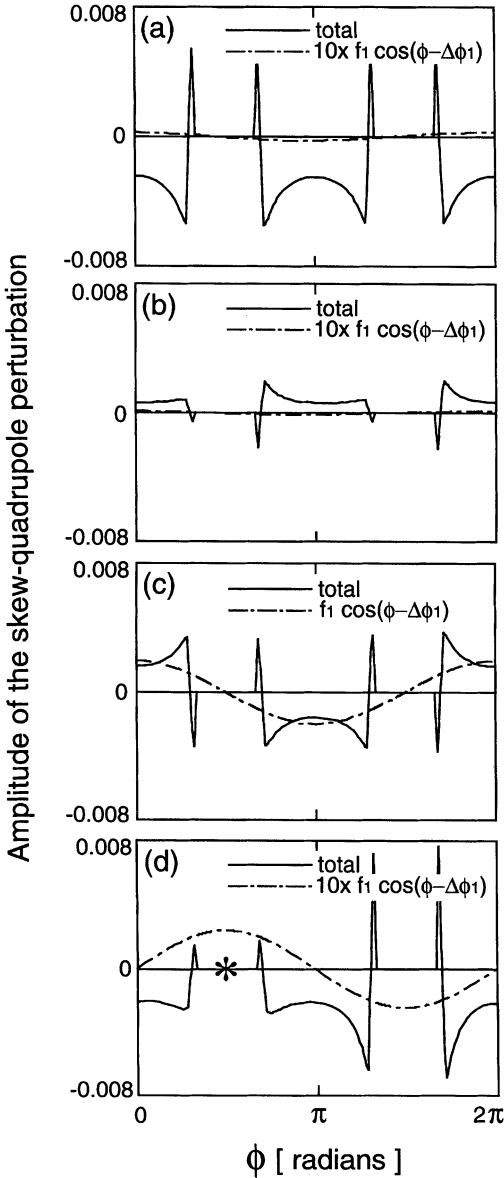FIGURE 7   Various closed orbits for the observation of beam profiles.

FIGURE 8   Skew-quadrupole perturbations originating from the various closed orbits in sextupole field of BMs without using correction coils. The phase $\phi = 0$ coincides with the center of BM1 in the real machine. (a) A-type, (b) B-type, (c) C-type, (d) D-type closed orbits. The symbol "∗" in (d) represents the location of the additional skew-quadrupole magnet for the coupling reduction in the D-type closed orbit.

equations:[1]

$$\alpha_x = \tan^{-1}\left(-\sqrt{\beta_y/\beta_x}\, d_{11} \tan \psi\right),$$
$$\alpha_y = \tan^{-1}\left(-\sqrt{\beta_x/\beta_y}\, d_{22} \tan \psi\right), \tag{12}$$

where α_x is the angle between the u axis and the x axis, and α_y between v and y. The parameters d_{11} and d_{22} are the elements of the matrix D defined as

$$D = \begin{pmatrix} d_{11} & d_{12} \\ d_{21} & d_{22} \end{pmatrix} = \frac{H}{\sqrt{\det H}}. \tag{13}$$

ψ is obtained by the following equation:

$$\tan 2\psi = \frac{-\sqrt{\det H}}{\frac{1}{2}\mathrm{Tr}(R(Q_x) - R(Q_y))}. \tag{14}$$

The summary of the $k = 1$ components and the estimated tilt angles at the monitor positions in BL2 and BL9 are shown in Table II. In the A- and B-type closed orbits, the $k = 1$ components are small; therefore, only small tilts are estimated. In contrast, the C- and D-type closed orbits introduce large $k = 1$ components; therefore, large tilts are estimated.

The coupling effect will be effectively reduced by suppressing the $k = 1$ component. For example, in the D-type closed orbit, we can

TABLE II Estimated $k = 1$ components of the skew-quadrupole perturbations and tilt angles of beam profiles α_x in calculation and experiment. The superscript "*" means that coupling reduction using a skew-quadrupole magnet is performed. The correction coils for sextupole field are not employed

Closed orbit	$k = 1$ skew-quad. component		Tilt angle α_x			
	$f_1 \times 10^4$	$\Delta\phi_1$ (radians)	Calculation (deg.)		Experiment (deg.)	
			BL2	BL9	BL2	BL9
A	0.250	−0.181	0.2	−2.1	0.0	3.0
B	0.100	−0.282	0.1	−0.9	0.0	−1.5
C	19.75	−0.018	−1.0	−63.3	−8.5	−37.5
D	2.414	1.545	−10.7	10.2	−19.0	38.0
D*	0.004	0.043	0.0	0.0	−1.5	0.0

obtain the following solution for the coupling reduction from Eq. (10):

$$k_{lens} = -\pi f_1 = -7.6 \times 10^{-4} \quad \text{and} \quad \phi_{lens} = \Delta\phi_1 = 1.545 \,(\text{radians}).$$
$$(15)$$

The ϕ_{lens} is represented by the "$*$" symbol in Figure 8(d) and corresponds to the position near the QF2 magnet in the real machine. Thus, the $k = 1$ component will be completely suppressed, as shown in Table II.

3.2.4 Observation of the Beam Profiles and Reduction of the Coupling Effect

We observed beam profiles with the same four vertical closed orbit distortions as described in the previous section. The experimental results are summarized in the last two columns of Table II. In these experiments, the correction coils for the sextupole field were not used. These experimental results qualitatively agree with the predicted ones in the previous section.

We then tried to eliminate the tilt of the beam profiles. In Super-ALIS, coupling reduction must be performed under the condition where the vertical closed orbit shows position monitor readings of zero. These restraints are requested by SR users whose beamlines are aligned by referring the geometry of the vacuum duct as a standard position. The requested closed orbit is obtained by reversing the sign of the reference orbit, and it is almost the same as the D-type closed orbit. In this closed orbit, the beam profiles before coupling reduction are seriously tilted as shown in Figure 9(a).

We tried two methods for eliminating the tilts of beam profiles in this closed orbit: reducing the sextupole field using correction coils, and suppressing the $k = 1$ component of the skew-quadrupole perturbation using a skew-quadrupole magnet. Beam profiles after employing the correction coils are shown in Figure 9(b). The beam profiles were still tilted, mainly because residual sextupole components exist at the edges even after employing the correction coils.

Figure 9(c) shows beam profiles after using a skew-quadrupole magnet located near a QF2 magnet. Using this magnet, we were able to make the beam profiles flat, even though the correction coils were
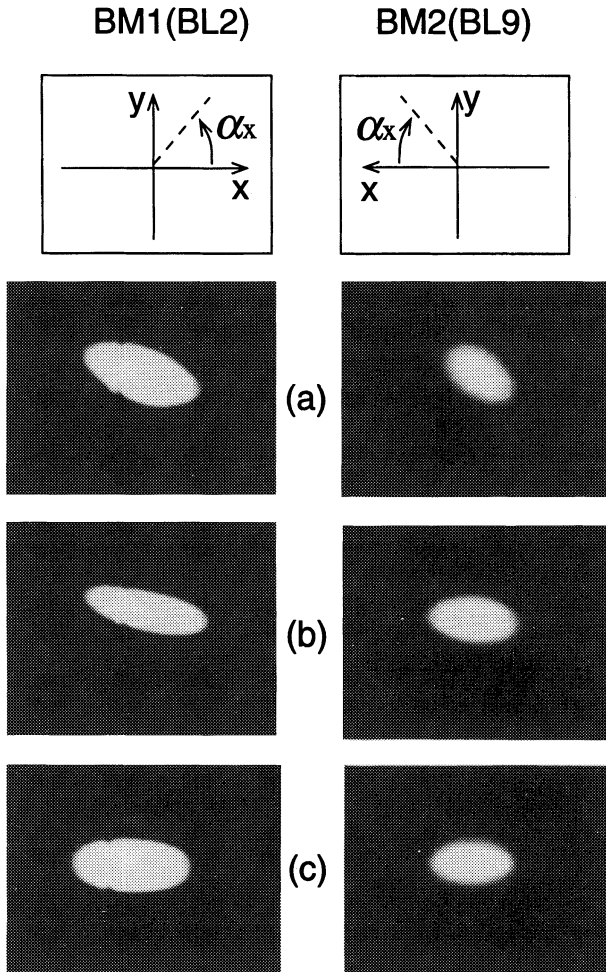
BM1(BL2)   BM2(BL9)

FIGURE 9   Experimental results in eliminating the tilt of beam profiles in the D-type closed orbit: (a) before coupling reduction, (b) using the correction coils for sextupole field, and (c) using a skew-quadrupole magnet (without using the correction coils).

not employed. The tilt angles observed after this coupling reduction are given in the last row of Table II. The strength of the additional skew-quadrupole magnet was $k_{lens} = -2.4 \times 10^{-3}$, which was about three times larger than the expected one. The origin of this disagreement is presently unclear. It may be due to the rough approximation of $\phi_x = \phi_y = \phi$ in the first stage of the theoretical approach.

4 CONCLUSION

We showed a coupling reduction method in which we only have to suppress the most harmful Fourier component of the skew-quadrupole perturbation. This method uses just one or two thin skew-quadrupole magnets; therefore, it should be a simple and effective method for coupling control in compact storage rings that have little space for correction instruments. The validity of this method was confirmed in experiments in a Super-ALIS machine. We effectively eliminated the tilts of the beam profiles originating from the vertical closed orbit in the sextupole field of bending magnets.

This kind of harmonic coupling reduction is similar to harmonic closed orbit correction;[11] therefore, it must have similar problems. Harmonic coupling reduction can greatly reduce the coupling effect all over the orbit; however, it cannot control the coupling arbitrarily because the coupling behavior varies along the ring in a given coupling condition. This defect might give rise to serious problems in high-brilliance third-generation storage rings that must ultimately reduce beam emittances. In these rings, therefore, the method should be used as a first step to the coupling reduction. However, in compact rings tuned generally for lithography in which precise coupling control is not necessary, the harmonic coupling reduction is enough for practical purposes.

References

[1] S. Peggs, *IEEE Trans. Nucl. Sci.* **NS-30**, 2460 (1983).
[2] P.J. Bryant, CERN ISR-MA/75-28.
[3] T. Hosokawa, T. Kitayama, T. Hayasaka, S. Ido, Y. Uno, A. Shibayama, J. Nakata, K. Nishimura and M. Nakajima, *Rev. Sci. Instrum.* **60**, 1783 (1989).
[4] T. Takayama and SHI Accelerator Research Group, *Rev. Sci. Instrum.* **60**, 1786 (1989).

[5] A.R. Jordan, R.J. Anderson, R.C. Lobel, A.S. Bhutta and D.E. Andrews, *Proc. of 1989 Intern. Symp. on MicroProcess Conference*, pp. 104–107.
[6] K. Yamada, T. Kaneko, K. Kuroda, M. Nakajima and T. Hosokawa, *Nucl. Instr. and Meth. B* **113**, 119 (1996).
[7] E. Courant and H. Snyder, *Ann. Phys.* **3**, 1 (1958).
[8] H. Wiedemann, *Particle Accelerator Physics II* (Springer-Verlag, 1995), pp. 29–38.
[9] H. Bruck, LA-TR-72-10 Rev, pp. 106–107 (1972).
[10] T. Kaneko, Y. Saitoh, S. Itabashi and H. Yoshihara, *J. Vac. Sci. Technol. B* **9**, 3214 (1991).
[11] E. Wilson, CERN 85-19, pp. 64–95 (1985).